

characteristic is practically without variation. Gain of 8 dBi and VSWR of less than 2 at 220-MHz frequency have been obtained. The concept of the presented antenna array may be used for frequencies from some hundreds of MHz to about 30 GHz.

#### ACKNOWLEDGMENTS

The authors are grateful to Ivana Radnovic, Milka Marjanovic, Momcilo Tasic, Zoran Micic, and Milica Rakic for their help with realization and measurement. This work was supported by the Serbian Ministry for Science, Technologies, and Development.

#### REFERENCES

1. K.-L. Wong, J.-W. Lai, and F.-R. Hsiao, Omnidirectional planar dipole-array antenna for 2.4/5.2-GHz WLAN access points, *Microwave Opt Technol Lett* 39 (2003), 33–36.
2. K.L. Wong, *Planar antennas for wireless communication*, Wiley, New York, 2003, p. 219.
3. M. Mikavica and A. Nestic, A. CAD for linear and planar antenna array of various radiating elements, Artech House, Norwood, MA, 1992.
4. H. Miyashita, H. Ohmine, K. Nishizawa, S. Makino, and S. Urasaki, Electromagnetically coupled coaxial dipole array antenna, *IEEE Trans Antenna Propagat* 47 (1999), 1716–1725.
5. A.D. Djordjevic, M.B. Bazdar, R.F. Harrington, and T.K. Sarkar, LINPAR, for Windows: Matrix parameters for multiconductor transmission lines, Software and user's manual, Version 1.0, Artech House, Norwood, MA, 1999.
6. IE3D, Zeland Software, Inc., Fremont, CA 4538, version 4.0.

© 2004 Wiley Periodicals, Inc. AQ1 Is "Zc" OK as is or make italic?

## DC-12-GHz 10-dB GAIN SHUNT-SERIES SHUNT-SHUNT WIDEBAND AMPLIFIERS BY COMMERCIALY AVAILABLE 0.35 $\mu\text{M}$ SiGe HBT TECHNOLOGY

C. C. Meng,<sup>1</sup> T. H. Wu,<sup>1</sup> and G. W. Huang<sup>2</sup>

<sup>1</sup> Department of Communication Engineering  
National Chiao Tung University  
Hsinchu, Taiwan, R.O.C.

<sup>2</sup> National Nano Device Laboratories  
Hsinchu, Taiwan, R.O.C.

Received 28 August 2003

**ABSTRACT:** The realization of wideband amplifiers with shunt-series shunt-shunt dual-feedback configuration with commercially available 0.35- $\mu\text{m}$  SiGe BiCMOS technology is reported. The SiGe HBT used here has  $f_t$  of 67 GHz and  $BV_{ce0}$  of 2.5 V. The experimental results show that power gain is 10 dB from DC to 12 GHz for a shunt-series shunt-shunt wideband amplifier, with the help of the emitter capacitive peaking technique. Input- and output-return losses are better than 10 dB for the same frequency range. Noise figure increases from 8 to 12 dB for frequencies from 1 to 18 GHz.  $OP_{1dB}$  and  $OIP_3$  are 0 dBm and 12 dBm at 1 GHz, respectively. Total current consumption is 11 mA at 3.3 V supply voltage. © 2004 Wiley Periodicals, Inc. *Microwave Opt Technol Lett* 40: 518–520, 2004; Published online in Wiley InterScience (www.interscience.wiley.com). DOI 10.1002/mop.20021

**Key words:** SiGe; HBT; amplifiers

#### INTRODUCTION

Wideband amplifiers [1–4] are used in a variety of modern communication systems. The Kukielka wideband amplifier is one of the most popular circuit topologies among all kinds of wideband amplifiers. The matched-impedance Kukielka wideband amplifier

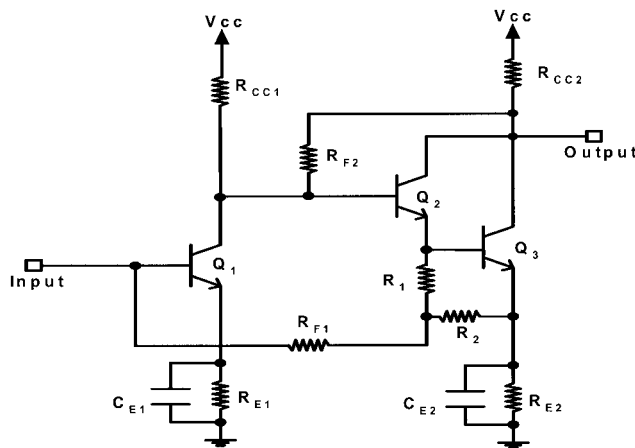


**Figure 1** Circuit schematic of the shunt-series shunt-shunt SiGe HBT wideband amplifier

is achieved by using a shunt-series shunt-shunt dual-feedback configuration. In this work, SiGe HBT Kukielka wideband amplifiers are demonstrated by a commercially available foundry service. The 0.35- $\mu\text{m}$  SiGe BiCMOS process is very economical because it is fabricated using the inexpensive I-line photolithography technique instead of the expensive deep-UV technique, and even the phase-shift mask photolithography technique is used for feature length of 0.25  $\mu\text{m}$  and below.

The circuit schematic of the designed shunt-series shunt-shunt SiGe HBT wideband amplifier is shown in Figure 1. A Darlington pair is used in the second stage to improve the frequency response. The resistors  $R_{F1}$  and  $R_{F2}$  in Figure 1 are the global feedback and local feedback resistors, respectively. The resistor  $R_{F1}$  is shunting at input and  $R_{F2}$  is shunting at output, in order to lower the terminal impedance to 50  $\Omega$  for the terminal impedance matching. The emitter peaking capacitors  $C_{e1}$  and  $C_{e2}$  are shown in Figure 1. The emitter capacitive peaking technique is used to overcome the

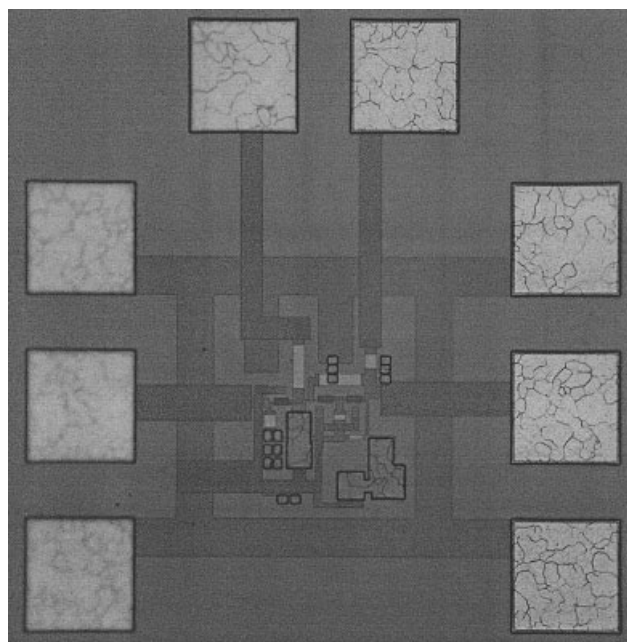


**Figure 2** Die photo of the shunt-series shunt-shunt dual feedback SiGe HBT wideband amplifier

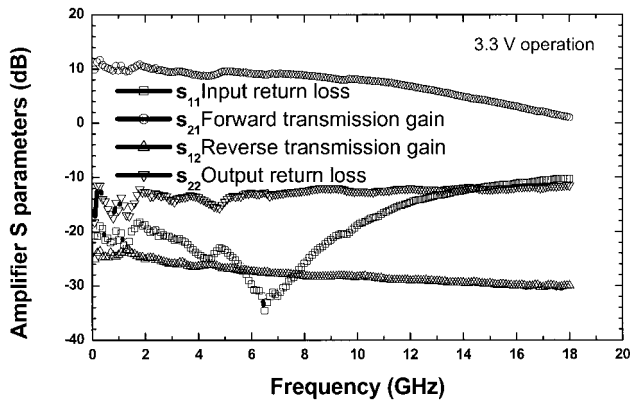


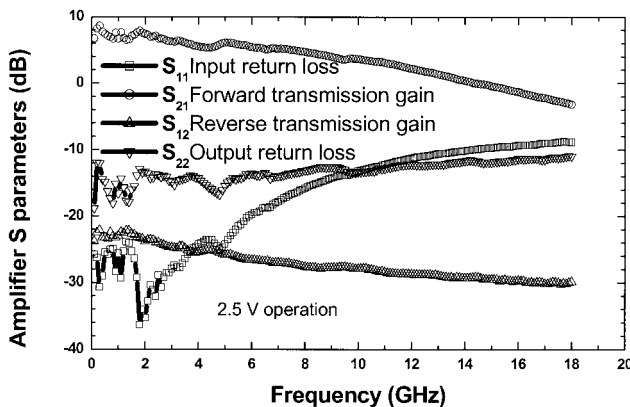
**Figure 3** Measurement results of the SiGe HBT wideband amplifier with  $V_{cc} = 3.3$  V and  $I_{total} = 11$  mA

intrinsic over-damped frequency response of the shunt-series shunt-shunt wideband amplifier and thus enhance the bandwidth [2, 5, 6]. The design principles of gain, bandwidth, and input/output return loss have been well established [5] for the shunt-series shunt-shunt wideband amplifier. Thus, 10-dB gain and input/output return loss of better than 10 dB are designed and demonstrated from DC to 12 GHz in this work.

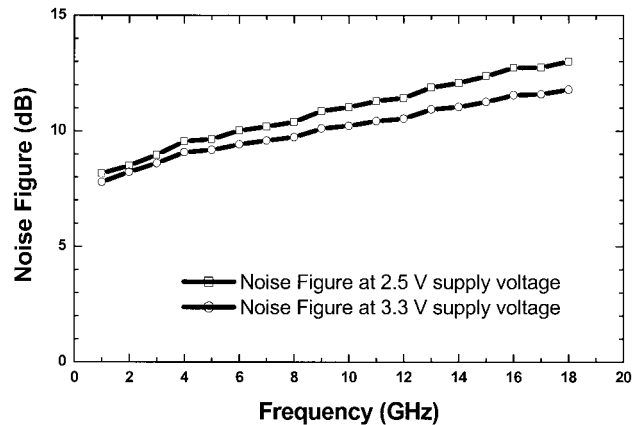
### MEASUREMENT RESULTS

Figure 2 illustrates the die photo of the fabricated SiGe HBT dual-feedback amplifier. The SiGe HBT device used here has  $f_t$  of 67 GHz and  $BV_{ceo}$  of 2.5 V. The amplifier has a coplanar ground-signal-ground pad to facilitate on-wafer probing. The size of all the SiGe HBT transistors in Figure 2 is  $0.3 \times 9.9 \mu\text{m}$ . The small emitter width reduces the intrinsic base resistance and intrinsic base-collector junction capacitor for higher  $f_{max}$ . The die size is  $0.7 \times 0.7$  mm. Most of the die area is not fully utilized to facilitate the on-wafer measurement and the die size of the wideband feedback amplifier can be easily compacted into  $0.4 \times 0.4$  mm.

The first stage consumes 3 mA and the second stage consumes 8 mA at 3.3-V supply voltage. Figure 3 shows the forward transmission gain, input-return loss, reverse transmission gain, and output-return loss for 3.3-V supply voltage. The shunt-series shunt-shunt dual feedback, SiGe wideband amplifier has 12 GHz of 3-dB gain bandwidth,  $S_{11}$  and  $S_{22}$  are below  $-10$  dB for the measurement range from DC to 18 GHz, as illustrated in Figure 3 for 3.3-V supply voltage.



**Figure 4** Measurement results of the SiGe HBT wideband amplifier with  $V_{cc} = 2.5$  V and  $I_{total} = 5$  mA



**Figure 5** Measured noise figures of the SiGe HBT wideband amplifier

The rf performance of the same SiGe wideband amplifier at 2.5-V supply voltage is also illustrated in Figure 4. The total bias current is 5 mA at 2.5-V supply voltage. The gain and bandwidth have been reduced to 8 dB and 8 GHz, respectively, as illustrated in Figure 4. Both bias conditions show that the terminal impedance matching is very good and the matching bandwidth is even higher than the 3-dB gain bandwidth.

Figures 5 and 6 illustrate the noise and power performances at both bias conditions. Noise performance is about one-half to one dB better at 3.3-V supply voltage. Noise figure increases from 8 to 12 dB for frequencies from 1 to 18 GHz at 3.3-V supply voltage.  $OP_{1\text{dB}}$  and  $OIP_3$  of the wideband amplifier, operating at 3.3-V supply voltage as a function of frequency, are illustrated in Figure 7.  $OP_{1\text{dB}}$  and  $OIP_3$  are 0 and 12 dBm at 1 GHz, respectively. Both  $OP_{1\text{dB}}$  and  $OIP_3$  decrease when the frequency becomes higher.  $OP_{1\text{dB}}$  and  $OIP_3$  become  $-9$  and 3 dBm at 12 GHz, respectively.  $OIP_3$  is about 12-dB higher than  $OP_{1\text{dB}}$  for the measured frequency range.

### CONCLUSION

This work has demonstrated a 10-dB gain DC–12-GHz SiGe HBT shunt-series shunt-shunt feedback wideband amplifiers by using a commercially available  $0.35\text{-}\mu\text{m}$  SiGe BiCMOS foundry. The total current consumption is 11 mA at 3.3-V supply voltage. The experimental results show that power gain is 10 dB and input/output return loss is below 10 dB from DC to 12 GHz for the wideband amplifier at 3.3-V supply voltage. Noise figure increases from 8 to 12 dB for frequencies from 1 to 18 GHz. Both  $OP_{1\text{dB}}$  and

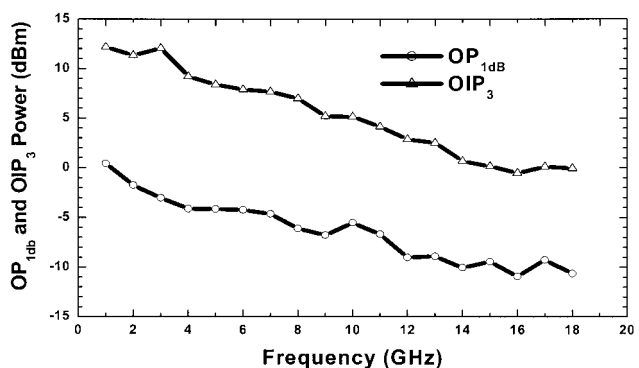


**Figure 6** Measured power performance of the SiGe HBT wideband amplifier at 3.3-V supply voltage

OIP<sub>3</sub> are a function of frequency. OP<sub>1dB</sub> and OIP<sub>3</sub> are 0 and 12 dBm at 1 GHz, respectively. Both OP<sub>1dB</sub> and OIP<sub>3</sub> decrease when frequency becomes higher. OP<sub>1dB</sub> and OIP<sub>3</sub> become -9 and 3 dBm at 12 GHz, respectively.

## ACKNOWLEDGMENTS

This work was supported by the National Science Council of Republic of China under grant no. NSC 92-2219-E-009-023 and by the Ministry of Education under grant no. 89-E-FA06-2-4. The authors also would like to thank the Chip Implementation Center in Taiwan for providing chip fabrication.

## REFERENCES

1. R.G. Meyer and R.A. Blauschild, A 4-terminal wide-band monolithic amplifier, *IEEE J Solid-State Circ* SC-16 (1981), 634–638.
2. C.D. Hull and R.G. Meyer, Principles of monolithic wideband feedback amplifier design, *Int J High-Speed Electron* 3 (1992), 53–93.
3. K.W. Kobayashi and A.K. Oki, A DC-10 GHz high gain-low noise GaAs HBT direct-coupled amplifier, *IEEE Microwave Guided Wave Lett* 5 (1995), 308–310.
4. K.W. Kobayashi and A.K. Oki, A Low-noise baseband 5-GHz direct-coupled HBT amplifier with common-base active input match, *IEEE Microwave Guided Wave Lett* 4 (1994), 373–375.
5. M.C. Chiang, S.S. Lu, C.C. Meng, S.A. Yu, S.C. Yang, and Y.J. Chan, Analysis, design, and optimization of InGaP-GaAs HBT matched-impedance wide-band amplifiers with multiple feedback loops, *IEEE J Solid-State Circ* 37 (2002), 694–701.
6. C.C. Meng, T.H. Wu, and S.S. Lu, 28-dB Gain DC-6GHz GaInP/GaAs HBT Wideband Amplifiers with and without Emitter Capacitive Peaking, *Euro Gallium Arsenide and other Semiconductors Appl Symp (GAAS 2002)*, 2002, pp. 311–314.

© 2004 Wiley Periodicals, Inc.

# AN ENHANCED CAVITY MODEL FOR MICROSTRIP ANTENNAS

Yeow-Beng Gan,<sup>1</sup> Chee-Pang Chua,<sup>2</sup> and Le-Wei Li<sup>2,3</sup>

<sup>1</sup> Tamasek Laboratories  
Singapore 119260

<sup>2</sup> Dept. of Electrical Computer Engineering  
National University of Singapore  
10 Kent Ridge Crescent  
Singapore 119260

<sup>3</sup> HPCES Program  
Singapore-MIT Alliance  
Singapore 119260

Received 21 August 2003

**ABSTRACT:** An enhanced cavity model for analyzing microstrip patch antenna is presented. The predicted resonant frequency and resonant resistance of the antenna are in good agreement with measured data. Theoretical results of the enhanced model are also compared with some commonly used models to determine their range of validity. © 2004 Wiley Periodicals, Inc. *Microwave Opt Technol Lett* 40: 520–523, 2004; Published online in Wiley InterScience (www.interscience.wiley.com). DOI 10.1002/mop.20022

**Key words:** cavity model; microstrip antennas; antenna analysis

## 1. INTRODUCTION

A conventional microstrip antenna is usually comprised of a metallic patch deposited on one side of the substrate and a ground plane on the other side. Over the years, many models [1–6] have

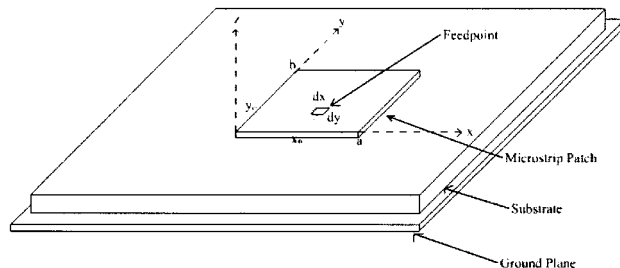


Figure 1 Rectangular microstrip patch antenna used in the experiment

been used to analyze microstrip patch geometry. Among them, the cavity model with perfect magnetic conducting (PMC) walls has been useful in providing insight regarding the radiation mechanisms of microstrip patch, but has also provided inaccurate prediction of its resonant frequency and resonant resistance. In this model, the thickness  $t$  of the microstrip patch antenna's substrate has been assumed to be electrically thin (usually on the order of  $0.01\lambda_0$ ) and a low dielectric constant has been used. These two assumptions made by the analytical models no longer hold because the microstrip patch antenna is increasingly used in the millimeter-wave region. To achieve miniaturization and larger bandwidth, thicker and higher dielectric substrate is also commonly used. Hence, a better analytical model or technique is needed to characterize the microstrip patch antenna.

## 2. ENHANCED MODEL

The enhanced cavity model is based on Carver and Coffey's [2, 3] design equations formulated for microstrip patch resonator using the modal-expansion technique. In this approach, the patch is viewed as a thin  $TM_z$ -mode cavity supporting quasi-discrete  $TM_{mn}$  modes transverse to  $z$ , where  $m$  and  $n$  are the mode numbers associated with the  $x$  and  $y$  directions, respectively. The field between the patch and the ground plane is expanded in terms of a series of eigenfunctions with their corresponding eigenvalues. For a nonradiating cavity, these eigenvalues are positive and real and are defined as  $k_x = n\pi/a$  and  $k_y = m\pi/b$ . For the cavity to radiate, the interior fields must be related to the exterior fields. This is achieved by imposing impedance boundary conditions at the four walls by making use of fictitious complex wall admittances  $Y_w$  to represent the external stored and radiated energy effects. Consider a microstrip patch antenna (shown in Fig. 1) of resonant length  $b$  ( $\approx \lambda_d/2$ ) along the  $y$  direction and width  $a$  ( $\approx 2b$ ), the following transcendental equation is obtained [3]:

$$\tan(k_y b) = \frac{2k_y \alpha_y}{k_y^2 - \alpha_y^2}, \quad (1)$$

where

$$\alpha_y = j \frac{2\pi\eta_0 t}{\lambda_0} \frac{Y_w F_y \left(\frac{a}{b}\right)}{a}$$

$$F_y = 0.7747 + 0.5977 \left(\frac{a}{b} - 1\right) - 0.1638 \left(\frac{a}{b} - 1\right)^2.$$

The wall admittance  $Y_w$  is multiplied by a factor  $F_y$  to take into consideration the effect of the aspect ratio  $a/b$  on the accuracy of the mode vectors used to represent the actual field distribution at the radiating edges. Better agreement between the predicted and measured results was found in comparison to  $F_y = 1$ . The wall